

Antiferromagnetism of $\text{Li}_2\text{Cu}_5\text{Si}_4\text{O}_{14}$ with alternating dimers and trimers in chainsG. Senthil Murugan,¹ P. J. Chen,² R. Sankar,^{1,2} I. Panneer Muthuselvan,¹ G. Narsinga Rao,¹ and F. C. Chou^{1,3,4,*}¹*Center for Condensed Matter Sciences, National Taiwan University, Taipei 10617, Taiwan*²*Institute of Physics, Academia Sinica, Taipei 11529, Taiwan*³*National Synchrotron Radiation Research Center, Hsinchu 30076, Taiwan*⁴*Taiwan Consortium of Emergent Crystalline Materials, Ministry of Science and Technology, Taipei 10622, Taiwan*

(Received 30 November 2016; revised manuscript received 4 May 2017; published 30 May 2017)

The crystal and spin structure of $\text{Li}_2\text{Cu}_5\text{Si}_4\text{O}_{14}$ [chemical formula $\text{Li}_2\text{Cu}_5(\text{Si}_2\text{O}_7)_2$] can be dissected into a copper spin chain system of alternating Cu_2O_2 dimers and Cu_3O_3 trimers linked with corner-shared oxygen and Si_2O_7 group in three dimensions (3D). The magnetic susceptibility (χ) and specific heat (C_P) measurement results suggest the existence of a magnetic ground state of 3D antiferromagnetic (AF) ordering with $T_N \sim 22$ K. Density functional theory (DFT) calculations have been applied to extract the exchange coupling constants for the ground-state spin structure. The calculated dominant intratrimer AF coupling ($J_1 \sim -9$ meV) and the intradimer ferromagnetic (FM) coupling ($J_3 \sim 1.8$ meV) supports that the copper spin-1/2 system evolves from a paramagnetic spin chain composed of alternating spin dimer and trimer to the 3D AF ordered ground state on cooling, and a weak frustration is proposed along the chain direction below T_N .

DOI: [10.1103/PhysRevB.95.174442](https://doi.org/10.1103/PhysRevB.95.174442)**I. INTRODUCTION**

Spin-1/2 magnetic insulators have attracted great attention due to their various intriguing magnetic properties of quantum nature, e.g., the spin-Peierls transitions in CuGeO_3 [1], the Bose-Einstein condensate in $\text{BaCuSi}_2\text{O}_6$ [2], and the skyrmions in Cu_2OSeO_3 [3]. In particular, the physics of carrier-doped CuO_2 plane has been explored extensively for the understanding of high- T_c superconductivity [4]. The spin-charge-phonon coupling of cuprate system depends sensitively on the dimensionality and coordination of the crystal structure, including the isolated copper spin in CuSe_2O_5 [5], the copper spin dimer in $\text{SrCu}_2(\text{BO}_3)_2$ [6], the copper spin trimer in $\text{La}_4\text{Cu}_3\text{MoO}_{12}$ [7], the odd-leg spin ladder in $\text{Sr}_2\text{Cu}_3\text{O}_5$ [8], the even-leg spin ladder in SrCu_2O_3 [9], the oxygen corner-sharing spin chain in Sr_2CuO_3 [10], the edge-sharing spin chain in Li_2CuO_2 [11], and the $\text{Na}_2\text{Cu}_5\text{Si}_4\text{O}_{14}$ with coexisting dimer and trimer in chains [12]. Here, we study the magnetic properties of $\text{Li}_2\text{Cu}_5\text{Si}_4\text{O}_{14}$ of coexisting spin dimer and trimer in chains in detail.

The symmetry of $\text{Li}_2\text{Cu}_5\text{Si}_4\text{O}_{14}$ has been described with the low symmetry space group $P\bar{1}$ (No. 2) due to its limited symmetry operations identified within the triclinic system [13]. The crystal structure consists of three kinds of Cu-O polyhedra which are linked through pyrosilicate groups of Si_2O_7 , and the Li atoms sitting in the interstitial sites ionically. The crystal structure, magnetic, and thermodynamic properties of the isostructural $\text{Na}_2\text{Cu}_5\text{Si}_4\text{O}_{14}$ have been studied before [12,14–16], including a weakly pronounced χT (susceptibility χ multiplied by the temperature) anomaly which has been suggested to signal the existence of a homometallic ferrimagnetic behavior with $T_N \sim 8$ K. However, we did not observe similar χT anomaly in $\text{Li}_2\text{Cu}_5\text{Si}_4\text{O}_{14}$ from this study, instead, a typical 3D AF spin ordering of $T_N \sim 22$ K is confirmed. In addition, a short range coupling indicated by a broad peak near ~ 8 K has been identified in both $d\chi(T)/dT$

and specific heat ($C_P(T)$), which suggests a weak reentrant spin frustration below T_N , and such reentrant frustration phenomenon has been proposed coming from the unique 1D frustration along the spin dimer-trimer chain direction based on the calculated magnetic exchange coupling constants. In this article, we report the physical properties of $\text{Li}_2\text{Cu}_5\text{Si}_4\text{O}_{14}$ through magnetic susceptibility and specific heat measurements. Spin exchange interactions have been calculated via DFT calculations and found consistent to the $\chi(T)$ data analysis.

II. EXPERIMENTAL AND CALCULATION DETAILS

Polycrystalline sample of $\text{Li}_2\text{Cu}_5\text{Si}_4\text{O}_{14}$ has been prepared by the solid state reaction method using Li_2CO_3 , CuO and SiO_2 of purity higher than 99.95%. The mixture of reagents was calcined at 700°C in the air for 48 hours, ground and sintered at 800°C and 900°C for 48 hours each with intermediate grindings. The phase purity and crystal structure were analyzed by the synchrotron x-ray powder diffraction (SXR) technique with energy of 20 keV (NSRRRC-Taiwan) at room temperature. The incident electron beam wavelength has been calibrated by the mixture of standard materials ($\text{LaB}_6 + \text{CeO}_2$) to have $\lambda = 0.62004$ (5) Å. The crystal structure was obtained as a result of Rietveld refinement under the Fullprof method on the SXR data. The magnetic measurements were performed using a superconducting quantum interference device vibrating-sample magnetometer (VSM) (Quantum Design, USA). The specific heat data were obtained using a standard relaxation method with a physical property measurement system (Quantum Design, USA).

The first-principles calculations based on the DFT were performed using QUANTUM ESPRESSO [17] with experimental structural parameters. The cutoff energy of the plane wave expansion is 40 Ry and a $10 \times 10 \times 8$ k mesh is used to sample the Brillouin zone. The DFT+ U scheme [18] with $U = 8.0$ eV and $J = 0.8$ eV is adopted to account for the localized nature of the Cu- d orbitals.

*Corresponding author: fcchou@ntu.edu.tw

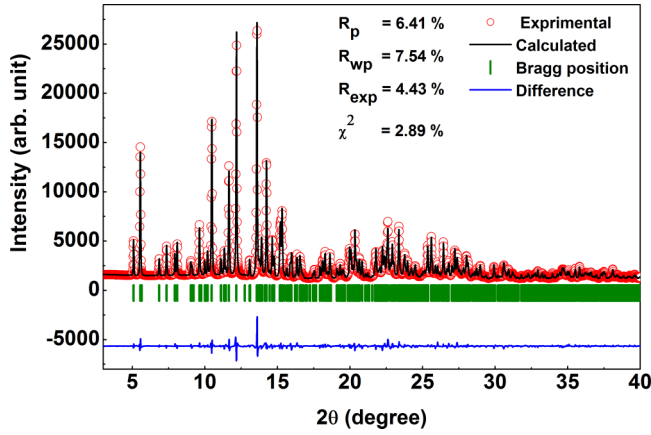


FIG. 1. The Rietveld refinement analysis for the powder x-ray diffraction pattern of $\text{Li}_2\text{Cu}_5\text{Si}_4\text{O}_{14}$, with Bragg peaks indexed with triclinic space group $P\bar{1}$. The open circles indicate the observed data and the Rietveld refinement fit is shown in black solid line. The Bragg positions and the difference curve are denoted by vertical green dashes and blue line, respectively.

III. RESULTS AND DISCUSSION

A. Crystal structure

Figure 1 shows the SXRD pattern of $\text{Li}_2\text{Cu}_5\text{Si}_4\text{O}_{14}$. The lattice parameters were refined using space group $P\bar{1}$ with Rietveld technique and the fitted values are $a = 7.4101(1)$ Å, $b = 7.7635(1)$ Å, $c = 5.4545(1)$ Å, $\alpha = 90.509(1)^\circ$, $\beta = 106.11(1)^\circ$, $\gamma = 114.70(1)^\circ$, and $V = 271.08(1)$ Å³, which are in good agreement with those published in the literature [13]. The refinement indicators to show the goodness of fit are $R_p = 6.41\%$, $R_{wp} = 7.54\%$, $R_{exp} = 4.43\%$, and $\chi^2 = 2.89\%$, respectively.

Figure 2 shows the polyhedral representation of $\text{Li}_2\text{Cu}_5\text{Si}_4\text{O}_{14}$ structure in 2D and 3D. The crystal structure can be viewed more clearly with the help of identifying a Cu-O plane composed of chains with alternating dimer and trimer. The Cu_2O_2 dimer and Cu_3O_3 trimer are linked through corner-shared oxygen and SiO_4 tetrahedra into a zigzag chain within each Cu-O plane, as shown in Fig. 2(a). These Cu-O planes are connected by the polyatomic groups of Si_2O_7 into a 3D structure, and Li atoms sitting in the interstitial sites as Li^+ ions, as shown in Fig. 2(b). The selected structural parameters for the Cu-O chain are listed in Table I, where the corresponding Cu and O sites are labeled in Fig. 2(a).

B. Magnetic susceptibility

Figure 3 shows the homogeneous dc magnetic susceptibilities ($\chi = M/H$) in $H = 100$ Oe for the $\text{Li}_2\text{Cu}_5\text{Si}_4\text{O}_{14}$ powder, no hysteresis was observed between the zero-field-cooled and field-cooled cycles. The $\chi(T)$ data show a cusp near ~ 22 K to indicate a typical paramagnetic (PM) to AF transition with $T_N \sim 22$ K. By plotting the $1/\chi$ versus T and extrapolating the linear fitting from high temperatures above 150 K, deviation from the linearity occurs below ~ 100 K and the x -intercept suggests Θ should be close to ~ -24 K. The $1/\chi$ deviation below ~ 100 K suggests that thermal energy of $k_B T \sim 100$ K is required to break the strongest spin exchange

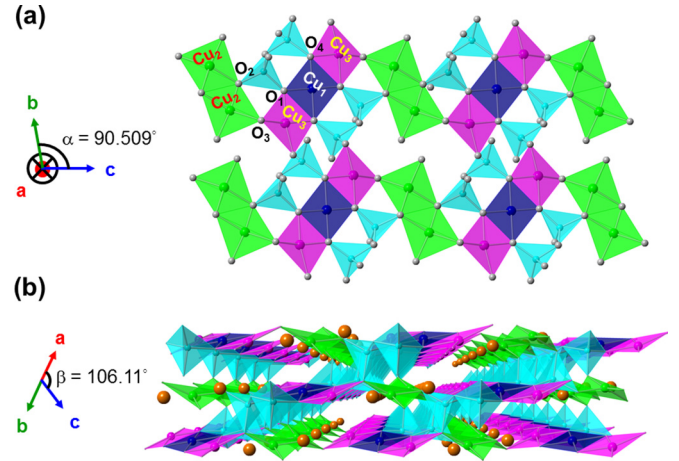


FIG. 2. The triclinic crystal structure of $\text{Li}_2\text{Cu}_5\text{Si}_4\text{O}_{14}$. (a) The copper spin dimers and trimers are linked in chains via corner-shared oxygen and SiO_4 tetrahedra to form a 2D plane projected along the a direction with $\alpha = 90.509^\circ$ shown. $\text{Cu}_2\text{-Cu}_1\text{-Cu}_3$ trimer and $\text{Cu}_3\text{-Cu}_1\text{-Cu}_3$ trimer are labeled, in accord with Table I. (b) These 2D planes are linked into a 3D structure through the corner-shared SiO_4 with Li atoms sitting in the interstitial sites. This nonorthogonal system is emphasized with $\beta = 106.11^\circ$.

coupling J . Thus Curie-Weiss law fitting with $\chi(T) = \chi_0 + C/(T - \Theta)$ has been applied to the high-temperature PM regime using data between 150-300 K. The fitted parameters return $\chi_0 = 5.67(1) \times 10^{-4}$ cm³ mol⁻¹, Curie constant $C = 2.22(1)$ cm³ K mol⁻¹, and Weiss temperature of $\Theta = -24$ K. The negative sign of Θ indicates the AF environment per spin under the molecular field approximation in the PM regime, which leads to the 3D AF spin ordering below T_N . On the other hand, the $\mu_{\text{eff}} = 1.88(1) \mu_B$ per Cu^{2+} calculated from the Curie constant is higher than the theoretical spin-only value of $1.73 \mu_B$ for Cu^{2+} ($S = 1/2$), which implies that orbital contribution is not quenched completely as a result of orbital hybridization between the d orbital of Cu and the p orbital of O.

The AF phase transition of $T_N \sim 22$ K has been verified with the signature of spin flop transition from the field

TABLE I. Selected refined structural parameters of Cu-O chain for $\text{Li}_2\text{Cu}_5\text{Si}_4\text{O}_{14}$. The copper and oxygen atoms for the dimer and trimer are labeled in Fig. 2(a).

Bond length (Å)	Bond angle (°)
dimer	
$\text{Cu}_2\text{-O}_2 = 1.9700$	$\text{Cu}_2\text{-O}_2\text{-Cu}_2 = 97.609$
$\text{O}_2\text{-Cu}_2 = 1.9207$	
trimer	
$\text{Cu}_3\text{-O}_4 = 1.9967$	$\text{Cu}_3\text{-O}_4\text{-Cu}_1 = 100.39$
$\text{O}_4\text{-Cu}_1 = 1.9092$	
$\text{Cu}_1\text{-O}_1 = 1.9549$	$\text{Cu}_1\text{-O}_1\text{-Cu}_3 = 100.11$
$\text{O}_1\text{-Cu}_3 = 1.9597$	
dimer-trimer	
$\text{Cu}_2\text{-O}_3 = 1.9823$	$\text{Cu}_2\text{-O}_3\text{-Cu}_3 = 114.16$
$\text{O}_3\text{-Cu}_3 = 1.9991$	

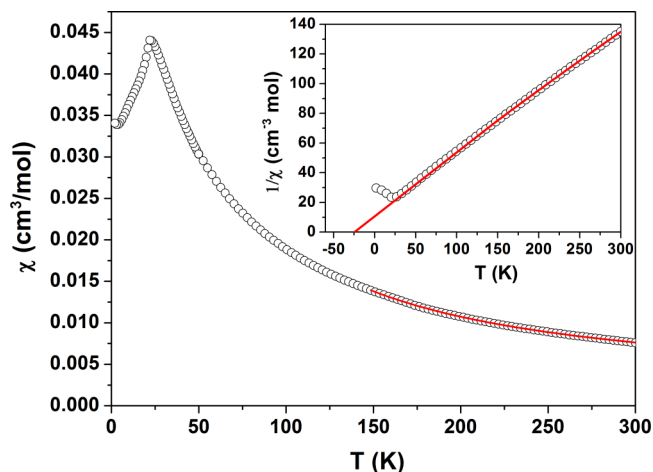


FIG. 3. The magnetic susceptibilities $\chi(T)$ of $\text{Li}_2\text{Cu}_5\text{Si}_4\text{O}_{14}$ measured under applied field of 100 Oe. The inset shows $1/\chi$ plot with a high temperature linear fitting that deviates from the linearity near ~ 100 K, and the Θ is extrapolated to -24 K. Curie-Weiss law fitting of $\chi = \chi_0 + C/(T - \Theta)$ used data between 150–300 K and is shown with solid line.

dependence of magnetization, as shown in Fig. 4. A magnetization jump near the critical field of $H_c \sim 27$ kOe can be identified below T_N , as also illustrated by the derivative dM/dH shown in the inset, which can be attributed to a spin-flop transition, i.e., a relatively weak on-site spin anisotropy is overcome by the high magnetic field so that the AF ordered spins are flopped perpendicular to the applied field direction [19].

C. Specific heat

Figure 5 shows the $C_p(T)$ for $\text{Li}_2\text{Cu}_5\text{Si}_4\text{O}_{14}$ measured in zero field. A λ -type peak is found near ~ 22 K, which indicates an entropy change as a result of AF phase transition and

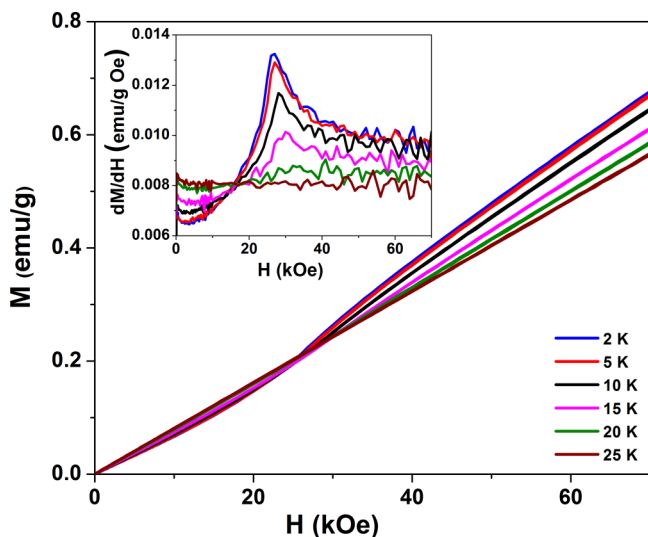


FIG. 4. Magnetization as a function of field for $\text{Li}_2\text{Cu}_5\text{Si}_4\text{O}_{14}$ for temperatures near and below T_N , the derivatives are shown in the inset.

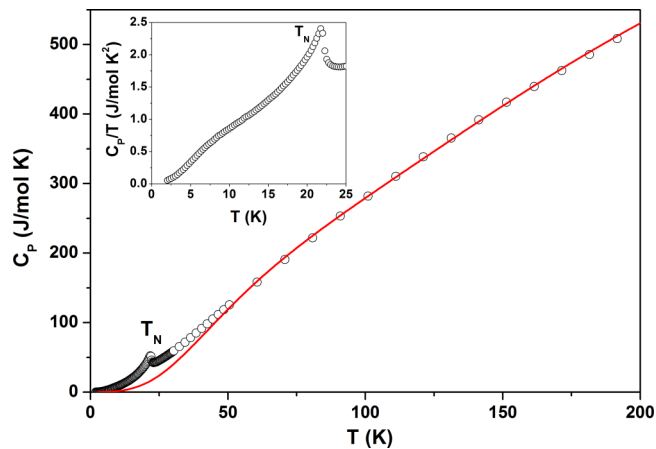


FIG. 5. The temperature dependence of specific heat (C_p) for $\text{Li}_2\text{Cu}_5\text{Si}_4\text{O}_{14}$ measured at zero field. The red solid line indicates a fit to the Debye model shown in Eq. (1). The inset shows the C_p/T vs T plot.

being consistent to the $\chi(T)$ measurement results (Fig. 3). To estimate the lattice contribution, we used a single Debye integral to fit the C_p data first, but it failed to give a satisfactory result. The best fit has been achieved via the linear combination of two Debye integrals, which is a reasonable choice for sample of different atomic masses per unit cell and the different normal modes correspond to the two different Debye temperatures [20,21]. C_p data between 50 to 200 K have been fitted to

$$C_{\text{phonon}}(T) = 9nR \sum_{i=1}^2 C_i \left(\frac{T}{\theta_{Di}} \right)^3 \int_0^{\theta_{Di}/T} \frac{x^4 e^x}{(e^x - 1)^2} dx, \quad (1)$$

where n is the number of atoms per formula unit, R is the gas constant, and θ_{Di} is the Debye temperature. The best fitting parameters are $C_1 = 0.35$, $\theta_{D1} = 248$ K, $C_2 = 0.9$, and $\theta_{D2} = 965$ K.

Since $\text{Li}_2\text{Cu}_5\text{Si}_4\text{O}_{14}$ is an insulator without significant electronic contribution, and the total specific heat includes contributions of magnetic and phonon origins, the magnetic specific heat (C_m) is extracted from subtracting the approximate lattice contribution from the total. The spin entropy change ΔS can thus be estimated from integrating the C_m/T with respect to temperature following $\Delta S = \int \frac{C_m}{T} dT$, as shown in Fig. 6. The spin entropy recovered at $T_N \sim 22$ K is about $15.73 \text{ J mol}^{-1} \text{ K}^{-1}$ which corresponds to $\sim 54.61\%$ of the total spin entropy, as estimated from the theoretical Dulong-Petit limit of $5R \ln(2S+1) \sim 28.81 \text{ J mol}^{-1} \text{ K}^{-1}$ ($R = 8.314 \text{ J mol}^{-1} \text{ K}^{-1}$) for Cu^{2+} of $S = 1/2$. These results suggest that nearly half of the spin entropy is lost above T_N due to the existence of short range coupling, as expected for a system composed of spin dimers and trimers in chains.

D. Calculated spin structure

The magnetic ground state and the corresponding exchange interaction constants have been calculated using the Heisenberg model $H = -\sum_{i,j} J_{ij} \mathbf{s}_i \cdot \mathbf{s}_j$. The definitions of the exchange couplings J_i 's with corresponding Cu-Cu distances are summarized in Fig. 7 and Table II, where J_1 and J_3

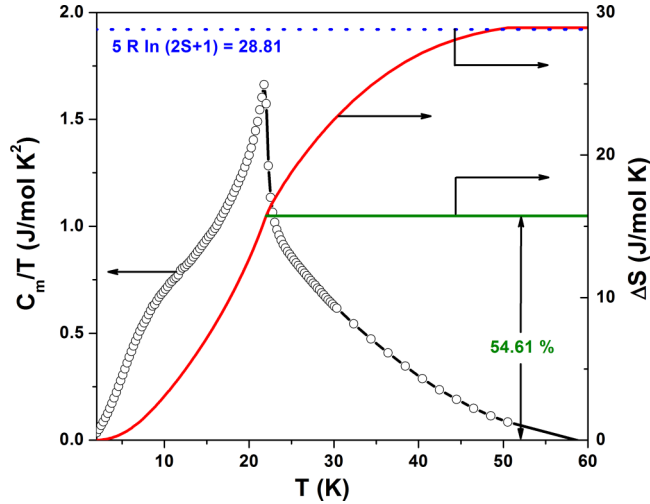


FIG. 6. Magnetic specific heat (C_m/T) for $\text{Li}_2\text{Cu}_5\text{Si}_4\text{O}_{14}$ is derived after the subtraction of phonon contribution using Debye model. Spin entropy change (ΔS) is shown in the inset as described in the text.

correspond to the intra-trimer ($\text{Cu}_3\text{--Cu}_1\text{--Cu}_3$) and intradimer ($\text{Cu}_2\text{--Cu}_2$) couplings, respectively. The total energies for six different spin configurations of various FM/AF intra- and interdimer/trimer couplings within $1 \times 1 \times 1$ unit cell were calculated relative to the nonmagnetic state as

$$\begin{aligned}
 (\uparrow\downarrow\uparrow\uparrow), E_1 &= -2J_1 + 2J_2 + J_3 + J_4 - 2J_5 + 2J_6, \\
 (\downarrow\uparrow\downarrow\uparrow), E_2 &= -2J_1 - 2J_2 + J_3 + J_4 + 2J_5 - 2J_6, \\
 (\downarrow\uparrow\downarrow\downarrow), E_3 &= -2J_1 + 2J_2 - J_3 + J_4 + 2J_5 - 2J_6, \\
 (\uparrow\uparrow\downarrow\downarrow), E_4 &= -2J_2 + J_3 - J_4 - 2J_5 - 2J_6, \\
 (\uparrow\uparrow\downarrow\uparrow), E_5 &= +2J_2 - J_3 - J_4 + 2J_5 + 2J_6, \\
 (\uparrow\uparrow\downarrow\downarrow), E_6 &= -2J_2 - J_3 - J_4 + 2J_5 + 2J_6.
 \end{aligned}$$

The total energies were calculated using DFT+ U method. The parameters ($U = 8.0$ eV and $J = 0.8$ eV) used in our calculations are within the common range for coppers spin-1/2 system of similar spin structure and insulating nature [22–24], which is believed that the main features of our systems can be captured reasonably well. In addition, we find that the antiparallel alignment between adjacent dimer-trimer groups of $(\uparrow\downarrow\uparrow\uparrow, \downarrow\uparrow\downarrow\downarrow)$ arranged in chain direction with $2 \times 1 \times 1$ supercell gives even lower energy, which is different from its isostructural $\text{Na}_2\text{Cu}_5\text{Si}_4\text{O}_{14}$ with the parallel arrangement of $(\uparrow\downarrow\uparrow\downarrow)$ groups in chain contributing to

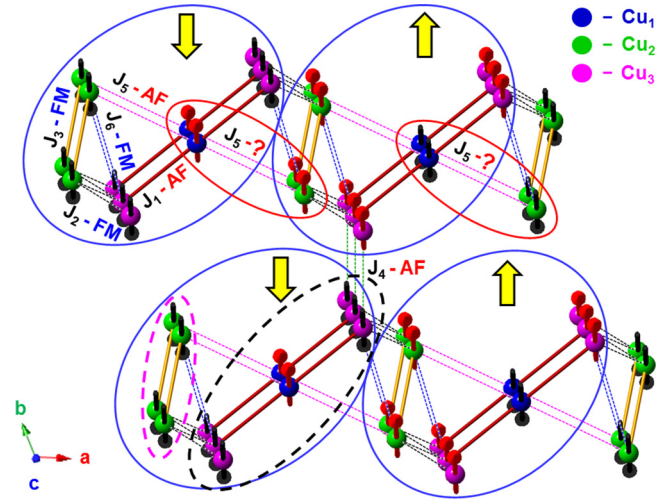


FIG. 7. The calculated spin structure of the ground state of $\text{Li}_2\text{Cu}_5\text{Si}_4\text{O}_{14}$. The exchange coupling constants J_i among $\text{Cu}_3\text{--Cu}_1\text{--Cu}_3$ trimer [Cu_1 (blue) and Cu_3 (magenta) in black dashed circle] and $\text{Cu}_2\text{--Cu}_2$ dimer (Cu_2 (green) in magenta dashed circle). The blue circle represents the dimer-trimer group and the red circle represents the weakly frustrated part of J_5 coupling connecting Cu trimer-dimer groups in 1D chain.

the nonzero ferrimagnetism [12]. This is one of the main contributions of this work. The calculated ground state is illustrated schematically in Fig. 7. The intratrimer coupling J_1 is AF, intradimer coupling J_3 is FM, and all other interdimer/trimer couplings are shown in Table II. The two dominant couplings are the AF intratrimer J_1 and the FM intradimer J_3 . A 3D AF spin structure has been constructed via the AF coupling of J_5 between two adjacent units of dimer-trimer group along the a -direction, and the weak AF coupling J_4 between adjacent trimers among dimer-trimer chains along the a direction. It should be noted that all four couplings of J_2 , J_4 , J_5 , and J_6 are contributing to the 3D AF ordering with alternating Cu trimer and Cu dimer.

From both the experimental and theoretical results, it is clear that the magnetic interaction of $\text{Li}_2\text{Cu}_5\text{Si}_4\text{O}_{14}$ at higher temperature region (above ~ 150 K) is dominated by the intra-trimer coupling J_1 . In addition, the size of intradimer coupling J_3 is close to the observed onset of a 3D AF ordering at $T_N \sim 22$ K. It is curious to find a broad $d\chi/dT$ anomaly appear near ~ 8 K below T_N at low field, as shown in Fig. 8. This $d\chi/dT$ anomaly is clearly field dependent, and has been confirmed by the ac susceptibility measurement in zero

TABLE II. Calculated exchange coupling constants J_i for $\text{Li}_2\text{Cu}_5\text{Si}_4\text{O}_{14}$.

Connection	Cu-Cu distance (Å)	J_i (meV)	J_i (K)
J_1 - Intratrimer	$\text{Cu}_3\text{--Cu}_1 \sim 3.0012$	-9.0	-104.44
J_2 - Interdimer/trimer	$\text{Cu}_2\text{--Cu}_3 \sim 3.3421/3.2641$	0.2	2.32
J_3 - Intradimer	$\text{Cu}_2\text{--Cu}_2 \sim 2.9278$	1.8	20.88
J_4 - Intertrimer	$\text{Cu}_3\text{--Cu}_3 \sim 3.2941$	-0.3	-3.48
J_5 - Interdimer/trimer	$\text{Cu}_2\text{--Cu}_1 \sim 3.6245$	-0.9	-10.44
J_6 - Interdimer/trimer	$\text{Cu}_3\text{--Cu}_1 \sim 3.7822$	0.8	9.28

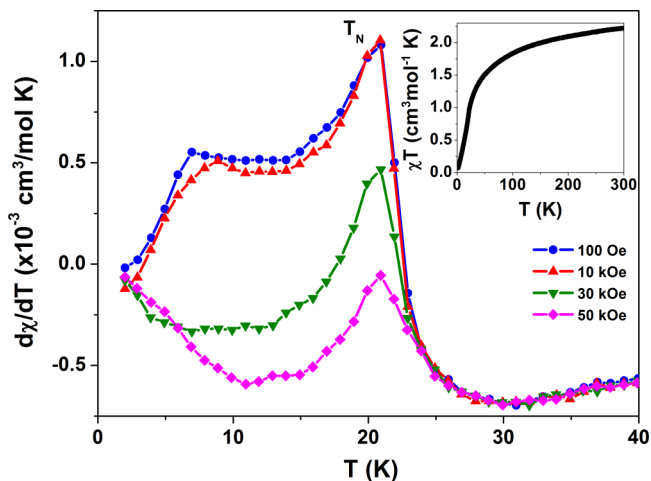


FIG. 8. The temperature dependence of $d\chi/dT$ for $\text{Li}_2\text{Cu}_5\text{Si}_4\text{O}_{14}$ at various applied magnetic fields. The inset shows the χT plot for $H = 100$ Oe.

applied field (not shown), but it is suppressed by field higher than ~ 10 kOe. We believe the observed $d\chi/dT$ anomaly below T_N could be related to the occurrence of spin frustration of low-dimensional nature.

Considering that the 3D AF spin ordering is the magnetic ground state, an additional long range spin ordering below T_N is unlikely, unless a structural distortion or additional spin-phonon coupling is developed below T_N . The broad peak of C_p/T (inset of Fig. 5) near 8 K indicates the enthalpy change due to a weak spin frustration mechanism. Although the deviation from the AF ground state is possible and has been found in compounds showing a reentrant spin glass behavior, i.e., disorder state emerges below the magnetically ordered state, the ac susceptibilities measured between 10–750 Hz do not show any frequency dependence (not shown) as a typical spin glass system, which suggests that the signature of weak frustration below T_N is not a typical reentrant spin glass phase transition [25]. We propose that frustration may occur between adjacent dimer-trimer groups along the a direction via J_5 coupling, as illustrated in Fig. 7. In particular, the estimated frustration factor $|\frac{J_5}{T_N}|$ is close to 1.1 only, which should not lead to a typical spin glass state of full frustration, but a weak spin frustration in 1D is possible.

E. Homometallic ferrimagnetism or not?

The existence of an anomaly in χT right before the 3D AF spin ordering has been interpreted as a signature of homometallic ferrimagnetism in $\text{Na}_2\text{Cu}_5\text{Si}_4\text{O}_{14}$ [12], i.e., a peculiar existence of residue FM moment for spins aligned antiferromagnetically for a homogeneous spin system. The main reason why homometallic ferrimagnetism was proposed in $\text{Na}_2\text{Cu}_5\text{Si}_4\text{O}_{14}$ could be closely related to the assumption that the distribution of copper $S = 1/2$ spins grouped in alternating dimer and trimer must be homogeneous in size and the AF spin alignment within each dimer-trimer group in $(\uparrow\downarrow\uparrow\downarrow)$ representation, which leads to a residue moment to indicate its ferrimagnetic nature [12]. On the other hand, we find that the $\text{Li}_2\text{Cu}_5\text{Si}_4\text{O}_{14}$ of similar crystal structure does not have the similar signature of χT anomaly above T_N to indicate the ferrimagnetism, as shown in the inset of Fig. 8. Instead, a perfect 3D AF ordering could be constructed via doubling of the dimer-trimer group along the a direction, as represented in $(\uparrow\downarrow\uparrow\uparrow\uparrow, \downarrow\uparrow\downarrow\downarrow\downarrow)$.

IV. CONCLUSIONS

In conclusion, the crystal and spin structure of $\text{Li}_2\text{Cu}_5\text{Si}_4\text{O}_{14}$ as a copper spin-1/2 system has been explored fully with susceptibility and specific heat measurements with supporting theoretical calculations. The spin system can be simplified having a magnetic ground state of 3D AF long-range ordering composed of alternating copper spin trimer and dimer grouped in chains with AF interchain coupling. Although $\text{Li}_2\text{Cu}_5\text{Si}_4\text{O}_{14}$ is isostructural to that of $\text{Na}_2\text{Cu}_5\text{Si}_4\text{O}_{14}$, the former has a stronger AF exchange coupling of higher T_N comparing to the latter without indication of homometallic ferrimagnetism. The calculated spin structure and measurement results suggest the existence of a novel low-dimensional spin frustration phenomenon below T_N , i.e., an reentrant behavior of weak frustration along the spin dimer-trimer chain direction.

ACKNOWLEDGMENTS

F.C.C. acknowledges support from the Ministry of Science and Technology in Taiwan under Project No. MOST-104-2119-M-002-028. We also acknowledge the useful suggestions provided by W. T. Chen on synchrotron XRD and B. Koteswararao on the specific heat data fitting.

- [1] M. Hase, I. Terasaki, and K. Uchinokura, *Phys. Rev. Lett.* **70**, 3651 (1993).
- [2] T. Giamarchi, C. Rugg, and O. Tchernyshyov, *Nat. Phys.* **4**, 198 (2008).
- [3] S. Seki, X. Z. Yu, S. Ishiwata, and Y. Tokura, *Science* **336**, 198 (2012).
- [4] B. Keimer, S. A. Kivelson, M. R. Norman, S. Uchida, and J. Zaanen, *Nature (London)* **518**, 179 (2015).
- [5] O. Janson, W. Schnelle, M. Schmidt, Yu. Prots, S.-L. Drechsler, S. K. Filatov, and H. Rosner, *New J. Phys.* **11**, 113034 (2009).
- [6] H. Kageyama, K. Yoshimura, R. Stern, N. V. Mushnikov, K. Onizuka, M. Kato, K. Kosuge, C. P. Slichter, T. Goto, and Y. Ueda, *Phys. Rev. Lett.* **82**, 3168 (1999).
- [7] M. Azuma, T. Odaka, M. Takano, D. A. Vander Griend, K. R. Poeppelmeier, Y. Narumi, K. Kindo, Y. Mizuno, and S. Maekawa, *Phys. Rev. B* **62**, R3588(R) (2000).
- [8] K. R. Thurber, T. Imai, T. Saitoh, M. Azuma, M. Takano, and F. C. Chou, *Phys. Rev. Lett.* **84**, 558 (2000).
- [9] M. Azuma, Z. Hiroi, M. Takano, K. Ishida, and Y. Kitaoka, *Phys. Rev. Lett.* **73**, 3463 (1994).
- [10] N. Motoyama, H. Eisaki, and S. Uchida, *Phys. Rev. Lett.* **76**, 3212 (1996).
- [11] Y. Mizuno, T. Tohyama, S. Maekawa, T. Osafune, N. Motoyama, H. Eisaki, and S. Uchida, *Phys. Rev. B* **57**, 5326 (1998).
- [12] M. S. Reis, A. Moreira dos Santos, V. S. Amaral, P. Brandao, and J. Rocha, *Phys. Rev. B* **73**, 214415 (2006).

- [13] K. Kawamura, A. Kawahara, and J. T. Iiyama, *Acta Crystallogr. Sect. B* **34**, 3181 (1978).
- [14] A. Moreira dos Santos, P. Brandao, A. Fitch, M. S. Reis, V. S. Amaral, and J. Rocha, *J. Solid State Chem.* **180**, 16 (2007).
- [15] M. S. Reis, A. Moreira dos Santos, V. S. Amaral, A. M. Souza, P. Brandao, J. Rocha, N. Tristan, R. Klingeler, B. Buchner, O. Volkova, and A. N. Vasiliev, *J. Phys.: Condens. Matter* **19**, 446203 (2007).
- [16] A. M. Souza, M. S. Reis, D. O. Soares-Pinto, I. S. Oliveira, and R. S. Sarthour, *Phys. Rev. B* **77**, 104402 (2008).
- [17] P. Giannozze *et al.*, *J. Phys.: Condens. Matter* **21**, 395502 (2009).
- [18] V. I. Anisimov, F. Aryasetiawan, and A. I. Lichtenstein, *J. Phys.: Condens. Matter* **9**, 767 (1997).
- [19] R. M. White, *Quantum Theory of Magnetism*, 3rd ed. (Springer, Berlin, 2007).
- [20] B. Koteswararao, R. Kumar, J. Chakraborty, B.-G. Jeon, A. V. Mahajan, I. Dasgupta, K. H. Kim, and F. C. Chou, *J. Phys.: Condens. Matter* **25**, 336003 (2013).
- [21] B. Koteswararao, S. K. Panda, R. Kumar, K. Yoo, A. V. Mahajan, I. Dasgupta, B. H. Chen, K. H. Kim, and F. C. Chou, *J. Phys.: Condens. Matter* **27**, 426001 (2015).
- [22] V. I. Anisimov, M. A. Korotin, A. S. Mylnikova, A. V. Kozhevnikov, D. M. Korotin, and J. Lorenzana, *Phys. Rev. B* **70**, 172501 (2004).
- [23] G. M. Lopez, A. Filippetti, M. Mantega, and V. Fiorentini, *Phys. Rev. B* **82**, 195122 (2010).
- [24] S. Pesant and M. Côté, *Phys. Rev. B* **84**, 085104 (2011).
- [25] J. A. Mydosh, *Spin Glass: An Experimental Introduction* (Taylor & Francis, London, 1993).